Pergamon

Cement and Concrete Research 32 (2002) 415–423

CEMENT AND CONCRETE RESEARCH

Monotonic and fatigue performance in bending of fiber-reinforced engineered cementitious composite in overlay system

Jun Zhang[a,*], Victor C. Li[b]

[a]*Department of Civil Engineering, Tsinghua University, Beijing 100084, China*
[b]*Advanced Civil Engineering Materials Research Laboratory, Department of Civil and Environmental Engineering, University of Michigan, Ann Arbor, MI 48109, USA*

Received 11 December 2000; accepted 25 September 2001

Abstract

This paper presents an experimental study and theoretical analyses on the monotonic and fatigue performance in bending of a polyvinyl alcohol (PVA) fiber-reinforced engineered cementitious composite (ECC) overlay system. The influence of the interfacial characteristics between overlay and old concrete substrate on the overall bending performance is investigated. The experimental results show that when ECC is used as overlay material, both load carrying capacity and deformability represented by deflection at peak load of the overlaid beams in flexure are significantly increased compared to those of plain concrete (PC) overlaid beams. The fatigue life of ECC overlaid beams in flexure is not influenced by the layer/base interfacial characteristics, such as smooth cutting surface or sand-blasted rough surface. However, the deformation ability of the overlaid beams, such as deflection at midpoint of beam, in both static and cyclic loading cases are influenced by the interfacial property. The smooth casting surface leads to larger deformation at peak load under monotonic loading and at failure under fatigue loading than the corresponding values for beams with a rough casting surface. The present study demonstrates that reflective cracking failure in pavement overlays can be eliminated by the use of a ductile material such as ECC.

Keywords: Overlaid pavements; Composite; Fatigue; Bending strength; Deformability

1. Introduction

Concrete pavements are popular for roads subjected to heavy traffic loads, such as highway networks and airfields, due to their high load carrying capacity and low maintenance requirement compared to flexible asphalt concrete pavements. Several hundred thousand kilometers of Portland cement concrete pavements had been built in US and in other countries in the past decades. At present, most of those concrete pavements are either approaching the end of their design lives or in need of repair [1]. For pavements subjected to moderate and heavy traffic, the most prevalent rehabilitating method is to place an overlay on the existing pavement. Asphalt concrete and Portland cement concrete are the most common materials to form the overlays. The overlays provide a smooth riding surface and strengthen the existing pavement, thus extending the pavement service life. However, a typical distress that occurs on those overlaid pavements is reflective cracking, which occurs when the existing cracks in the underlying pavements reflect into the newly constructed overlay under traffic loads. Cracking in overlay slabs reduces the load capacity and may result in fatigue failure [2–5]. In addition, cracks allow water and other chemical agents, such as deicing salts, to go through the cover layer to come into contact with the reinforcement, leading to reinforcement corrosion and rupture. Cracks in the top layer of a pavement may cause pumping of soil particles through the cracks, thus reducing the soil load bearing capacity. Also, severely spalled and wide cracks will increase the roughness of the pavement and reduce its serviceability to the motorist and also result in discomfort for users, finally leading to service termination.

The deterioration of concrete overlays is caused by concrete shrinkage, temperature changes, freeze and thaw cycles

* Corresponding author. Tel.: +86-10-62785836; fax: +86-10-62771132.
E-mail address: junz@tsinghua.edu.cn (J. Zhang).

0008-8846/02/$ – see front matter © 2002 Elsevier Science Ltd. All rights reserved.
PII: S0008-8846(01)00695-0

and repeated truck loading. The various stages of concrete overlay deterioration may be summarized as follows:

(1) Initial cracks due to shrinkage and temperature changes and traffic loading: Concrete shrinks as the cement paste hardens. If a concrete slab of moderate dimensions rests freely on its supports, it can contract to accommodate the shortening of its length produced by shrinkage. However, in the overlay system, concrete overlay and old pavement are in contact with each other and the overlay cannot contract freely. Thus, as overlaid concrete shrinks, a certain amount of tensile stresses will be developed in the overlay. The resulting tensile stresses in concrete due to shrinkage and restraints from connected members are known as shrinkage stresses. A change in temperature may have an effect similar to shrinkage, which also results in stresses in the overlaid slab, with increasing temperature results in compressive stresses and decreasing temperature results in tensile stresses. The stresses caused by shrinkage and temperature changes are illustrated in Fig. 1.

Traffic loading over pavement induces bending stresses in the slab. Due to the influence of existing cracks in old pavement (no load transfer through the existing cracks), the bending stresses in the overlay achieve the maximum value at and/or close to the existing cracked section, i.e., in or close to the cross-section of existing cracks. In addition, due to the difference in deformation behavior between new constructed overlay and old pavement, a certain delamination along the interface of overlay and old pavement starting from the existing cracks will take place. Therefore, the above maximum bending stress zone is extended to both sides from the existing cracks to the endpoints of the delamination zone on each side. The bending stresses caused by traffic loading are shown in Fig. 2.

As the tensile stress produced by shrinkage and/or temperature changes and traffic loading attains the tensile strength of the overlay material, cracking occurs. These cracks are known as reflective cracks in overlaid pavements. Generally, these reflective cracks are present around existing cracks in the old pavement due to above-stated reasons. It should be clearly understood that stresses caused by concrete shrinkage and temperature changes are independent of applied loads. However, load stresses in addition to

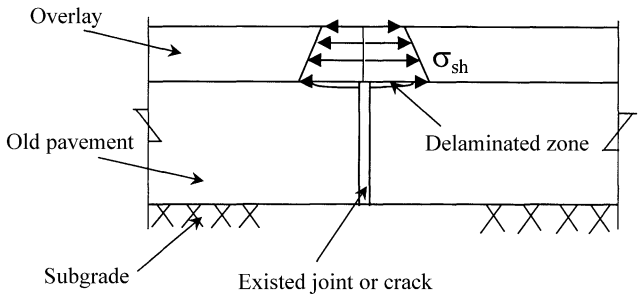

Fig. 1. Shrinkage- or temperature-induced tensile stresses in concrete overlay.

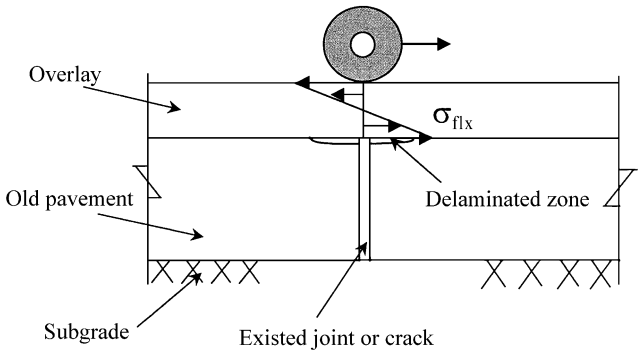

Fig. 2. Flexural stresses in concrete overlay caused by moving traffic load.

restrained movement stresses, including thermal warping stress, may reach to such an extent that the overlay cracks. It is also realized that under certain prevalent conditions, the shrinkage and temperature stresses may exceed in magnitude stresses produced by the heaviest traffic loads. In some cases, the shrinkage or temperature change-induced stresses alone are large enough to crack the overlay.

(2) Formation of through-thickness reflective cracks: These reflective cracks are subjected to freeze and thaw cycles. For example, in Michigan, there are about 10 freeze–thaw cycles per year [6]. Freezing water expands and results in additional damage, increase of crack width and depth. Cracking in slab surface is exacerbated by traffic loads. Each passage of a heavy wheel may causes a strain/stress concentration, which leads to further cracking and disintegration of the slabs. In addition, further development of concrete shrinkage or temperature change also leads to the growth of the transverse cracks. These combined factors leads to the formation of through-thickness cracks.

(3) Water penetration and wearing out of the through cracks and final failure in shear, delamination and spalling: Water gradually moves downward through the cracks. Under repeated traffic load, the through crack faces are gradually worn out, leading to the loss of load distribution in the longitudinal direction. As a result, the overlay slab does not behave as a plate any longer but acts as transverse beam. The presence of water accelerates the wearing out procedure. Finally, passages of truck wheels on the cracked overlay result in severe spalling, reducing or terminating the ability to carry traffic.

The above studies indicate that in overlaid pavements, the initial shrinkage and/or temperature change and traffic loading-induced reflective cracking and subsequent through slab-thickness crack propagation under repeated traffic load are the principal reasons for limiting the service life of the structures. Therefore, the prevention of reflective cracking in overlaid slabs is crucial, and the sequence of deterioration stages described above has to be interrupted before final pavement failure. Hence, reducing shrinkage crack width and enhancing fatigue crack growth resistance of the material become critical objectives to prolong the service life of the overlaid pavements.

To realize the above target, two approaches can be followed. First, if the deformation capacity of the material used in the overlay can be increased above that of plain concrete (PC; 0.01% ultimate tensile strain), the strain energy produced by shrinkage (under restrain condition) and temperature change can be released by the high deformation capacity of the material without reducing load carrying capacity. Second, the load carrying capacity of the overlaid pavement has to be increased so that the fatigue resistance of the structure can be improved under given traffic loading condition.

In the present paper, a laboratory experimental investigation on the application of polyvinyl alcohol (PVA) fiber-reinforced engineered cementitious composite (ECC) in the overlaid pavements was carried out. ECC is a cement-based composite reinforced with a few volume percentage (usually less than 3%) of short randomly oriented fibers. The composite has been microstructurally engineered to strain harden via multiple cracking in uniaxial tension [7,8]. ECC exhibits macroscopic strain hardening after first crack. The use of ECC for concrete repair was proposed by Li et al. [9] and some work on this subject has been done in the previous studies by using polyethylene (PE) fibers as reinforcement [10,11]. However, the performance of PVA fiber-reinforced ECC in repair, especially the fatigue performance of ECC overlaid beams, is not understood at present time. Also, this understanding is critically needed to use the ECC in overlaid pavements. The present paper focuses on the monotonic and fatigue performance of PVA fiber-reinforced ECC overlaid beams under flexural loading. The influence of interface characteristics between ECC overlay and existing concrete beams is studied. Two kinds of substrate casting surface, i.e., a smooth diamond saw cut surface and a sand-blasted surface, were prepared. As control specimens, beams with conventional PC material as overlay were cast and tested as well. Failure mechanism and theoretical analyses are given following the presentation of the experimental results.

2. Experimental program

2.1. Test specimen and loading conditions

To simulate the reflective cracking in overlaid pavements, a composite beam, initially used by Lim and Li [10] and Kamada and Li [11], is employed with four-point bending load applied to the beam as a general loading condition. The specimen includes a vertical crack introduced in the old concrete substrate and an initial interfacial crack between overlay and old concrete substrate in the center of the beam. The deflection is carefully monitored during testing using a reference beam attached to the top of the beam by three steel blocks glued to the beam surface. Two linear variable differential transducers (LVDTs) mounted on both sides of the center of the beam are used for measuring the deflection. The loading configuration and dimensions of the specimen are shown in Fig. 3A and the whole experimental set-up is shown in Fig. 3B.

For monotonic flexural tests, the tests were conducted with deformation controlled by the displacement of the actuator. The displacement was increased at a constant rate of 0.10 mm/min according to ASTM C1018. For fatigue tests, one-stage constant amplitude fatigue loading was used. The tests were carried out in load control using a sinusoidal waveform with a frequency of 1–2 Hz. A constant ratio R between minimum and maximum load

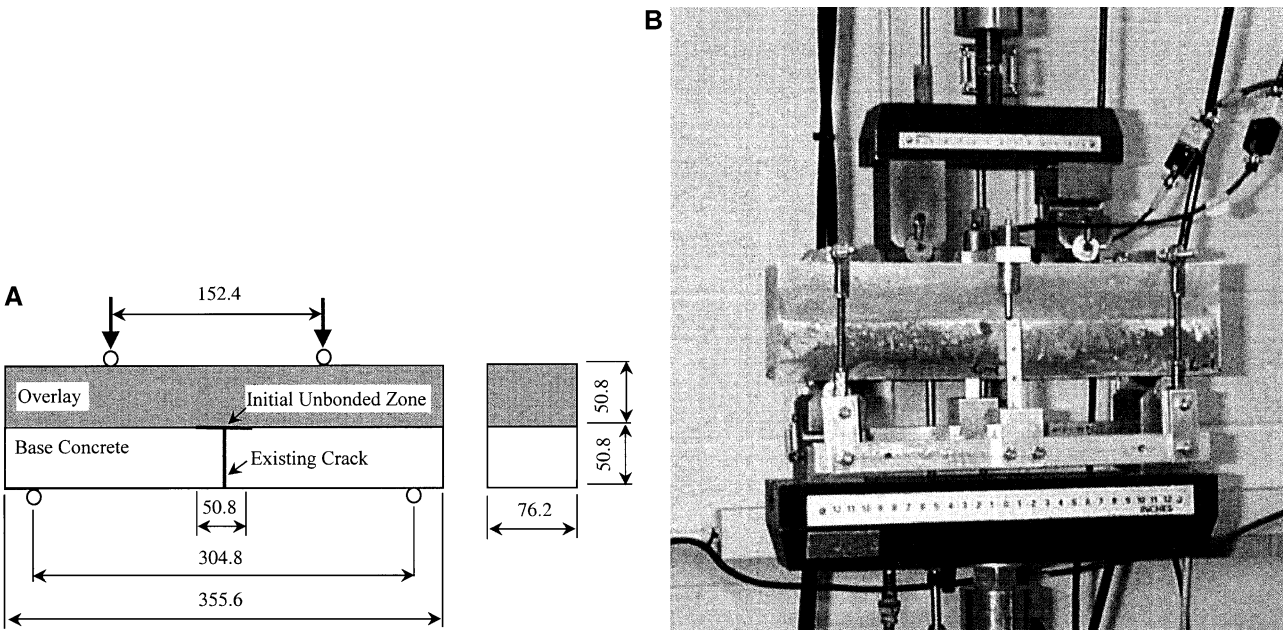

Fig. 3. (A) Dimension of composite beam and loading configuration in bending (mm) and (B) test set-up.

Table 1
Mix proportions of PC and ECC

Components	PC	ECC
Cement	1.00	1.00
Sand	1.62	1.00
Stone	1.62	–
Water	0.45	0.434
Superplasticizer[a]	0.005	0.025
Methyl cellulose	–	0.002
PVA fibers	–	2% in volume

[a] The water content in the superplasticizer is 66%.

levels ($R = P_{min}/P_{max} = 0.1$) and a varying maximum load level (P_{max}) were used in the present test program. The fatigue test commenced with a ramp to the maximum load P_{max} at a rate of 0.1 kN/s followed by a sine waveform fatigue loading in load control. The raw data consisted of time, load, actuator position and deflection readings from each LVDT. All of the tests were performed in a 250-kN load capacity, MTS-810 testing machine equipped for closed-loop testing.

2.2. Details of materials and specimen preparation

In the present investigation, ASTM Type I ordinary Portland cement, natural river sand with approximate particle size 0.3–4 mm and crushed natural stone with maximum particle size 10 mm were used in the substrate concrete beam. For the ECC overlay, ASTM Type I ordinary Portland cement and fine silica sand with approximate particle size 0.1–0.2 mm were used to form the matrix. PVA was employed as the fiber reinforcement. The mix proportions of PC and ECC adopted in this study are given in Table 1. The fiber properties are listed in Table 2. The design of the PVA-ECC material is described in Li et al. [12].

The base concrete blocks were cut out of concrete beams with size 356 × 76 × 102 mm. These concrete beams were cast and demolded 24 h after casting. After demolding, the beams were cured in water at 23 °C for 4 weeks and then were cut into the base blocks with a diamond saw. Each such beam was cut into four blocks with height 50.8 mm to form two substrate beams with preinduced joint (or substrate crack) at beam center. These blocks were kept in laboratory condition for another week before the overlay was cast. Two types of casting surface against the overlay were prepared in this study. One was the simple diamond saw cut surface and the other was the cut surface subjected to sand blasting. The initial interfacial crack and joint were made by using a smooth tape on the substrate blocks prior to casting the overlay material. The specimen preparation procedures are shown in Fig. 4.

Table 2
Properties of fiber used in this study

Type	E_f (GPa)	σ_f (MPa)	d_f (mm)	L_f (mm)
PVA (K-II)	42.8	1620	0.039	12

E_f: fiber modulus; σ_f: fiber tensile strength; d_f: fiber diameter; L_f: fiber length.

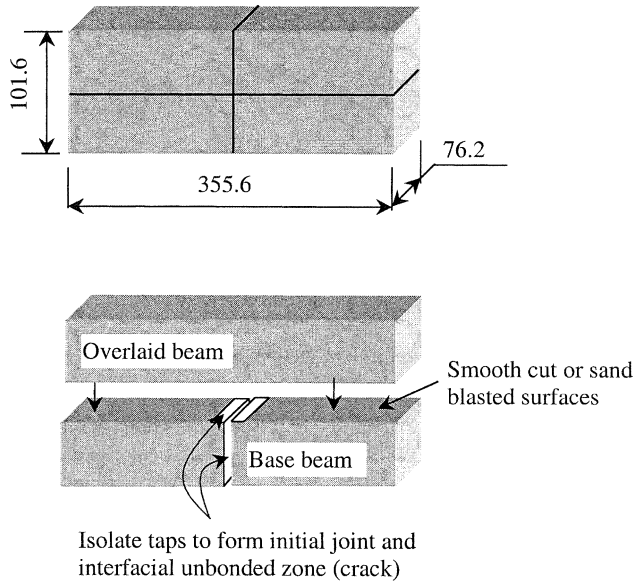

Fig. 4. Specimen preparation procedures.

The composite beams were demolded 24 h after the overlay was cast and were cured under water at 23 °C for 4 weeks. Then, the specimens were dried for another 2 weeks in air before testing. As control, specimens with PC as overlaid material were cast also at the same time.

A Hobart-type mixer was used to prepare the fresh materials. For PC, the mixing time was 5 min. For ECC, 10-min mixing time was used to ensure good fiber distribution in the matrix.

3. Experimental results and discussion

3.1. Flexural performance under monotonic loading

The monotonic flexural behavior of the composite beams is shown in Fig. 5 in terms of flexural stress

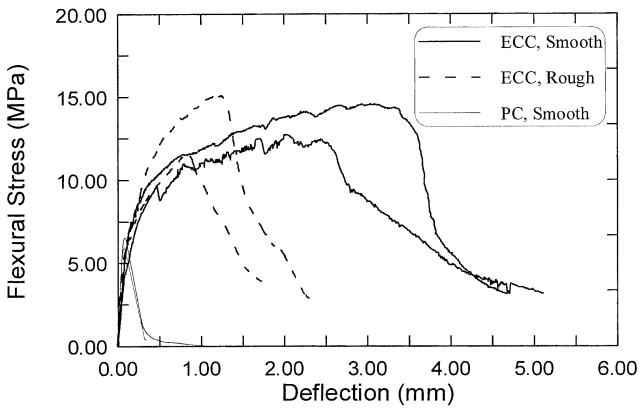

Fig. 5. Flexural stress and midpoint deflection diagrams of composite beams under static bending load.

Table 3
Performance parameters of the overlaid beams under static flexural load

Specimen types	First cracking strength (MPa)	MOR (MPa)	Model-predicted MOR (MPa)	Deflection at MOR (mm)
PC overlay with smooth interface	5.2	(6.53, 5.95) 6.24	6.93	(0.070, 0.079) 0.075
ECC overlay with rough interface	3.5	(15.12, 11.57) 13.35	13.87	(0.83, 1.20) 1.05
ECC overlay with smooth interface	3.5	(14.58, 12.77) 13.68	13.87	(2.45, 2.03) 2.24

midpoint deflection diagrams. The flexural stress F is the maximum tensile stress at the base of the overlay above the joint as determined from moment M using simple linear elastic theory:

$$F = \frac{M}{\frac{1}{6}Bh^2} \quad (1)$$

where B and h denote the width and the depth of the overlay (Eq. (1)). The dimensions of the overlay are used because there was no load transferred through the vertical joint. The corresponding flexural strength (MOR) and the deflection at peak flexural stress are listed in Table 3. The typical crack patterns at failure of the beams with different overlay material (PC and ECC) and different interfacial characteristics (smooth cut surface and rough sand-blasted surface) are shown in Fig. 6. The delaminated length along the interface of overlay and base concrete measured after testing in all testing cases is shown in Fig. 7.

Examining the complete flexural stress–deflection curves, significant differences between PC overlay and ECC overlay with different interface characteristics can be noted. First, it is clear that the bending load carrying capacity of the composite beams is significantly increased by using the ECC material in the overlay (above 100% of the value of PC overlaid beam). Similar results were obtained from the previous work by using PE fiber-reinforced ECC [10,11]. Second, the deformation capacity, represented by midpoint deflection at peak load of the beams with ECC overlaid, is obviously increased in comparison to that of PC overlaid beams. The difference between PC and ECC overlaid beams on the deformability is due to the single cracking behavior of PC in bending and the multiple cracking behavior of ECC in bending, respectively. These performance differentials including load carrying capacity and deformation capacity are principally a result of the difference of the stress–crack opening ($\sigma-\delta$) relationship of the materials [8,13,14]. Detailed analyses on this aspect are given in Section 4. Third, by comparing the deflection at peak load in the smooth and rough interface cases of ECC overlaid beams, we can see that the smooth interface can raise the deformation level of the composite beam. That is because the smooth interface allows extension of the delaminated length along the interface between ECC and concrete base under bending load, thus allowing more bending cracks to occur in the overlay. This means that the multiple cracking zone is extended. This phenomenon was also found in the previous work by Kamada and Li [11] using PE fiber as fiber reinforcement. This finding is useful in overlaid pavement design with application of fiber-reinforced cementitious composites in the layer. It should be noted that there is no influence of the overlay/substrate interfacial characteristics on the deformation ability of PC overlaid beam (see Ref. [11]) due to the low cracking resistance and single cracking behavior in tension of PC material. Fourth, from Fig. 5, it can be concluded that the influence of the interfacial property on the load carrying capacity of the ECC overlaid beams is

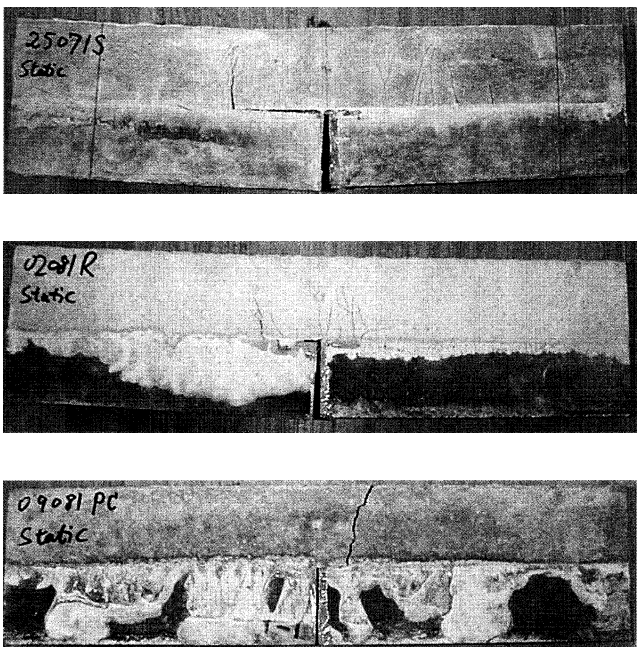

Fig. 6. Crack patterns at failure of overlaid beams under static bending load: (a) ECC overlay with smooth casting surface, (b) ECC overlay with rough casting surface and (c) PC overlay with smooth casting surface.

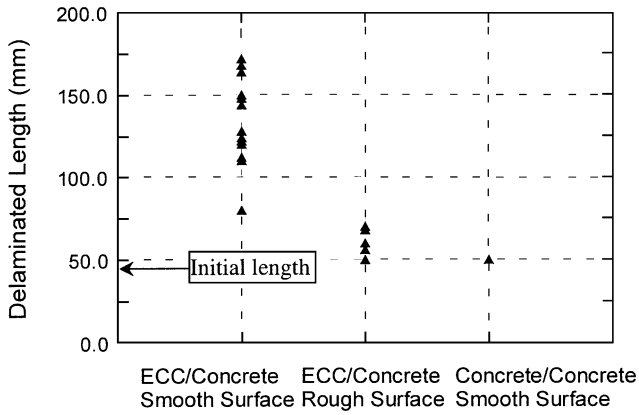

Fig. 7. Interfacial delaminating length in different types of beams under static bending load.

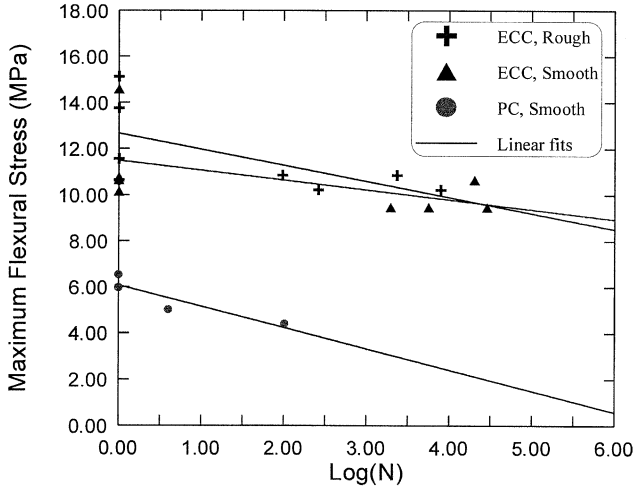

Fig. 8. Maximum flexural stress and fatigue life relations of the overlaid beams with different overlay materials and interface characteristics.

almost negligible. The average MOR in the smooth and rough interface cases is 13.68 and 13.35 MPa, respectively. The similar bending strength is associated with a single dominant flexural crack in the beam, controlled by the crack bridging behavior ($\sigma-\delta$ relation) of bridging fibers [13,14]. On the other hand, the ECC/concrete interfacial property influences the length of the delaminated zone, which in turn controls the deformation capacity of the beam.

3.2. Flexural performance under fatigue loading

The fatigue performance in bending of the overlaid beams is shown in Fig. 8 in terms of maximum flexural

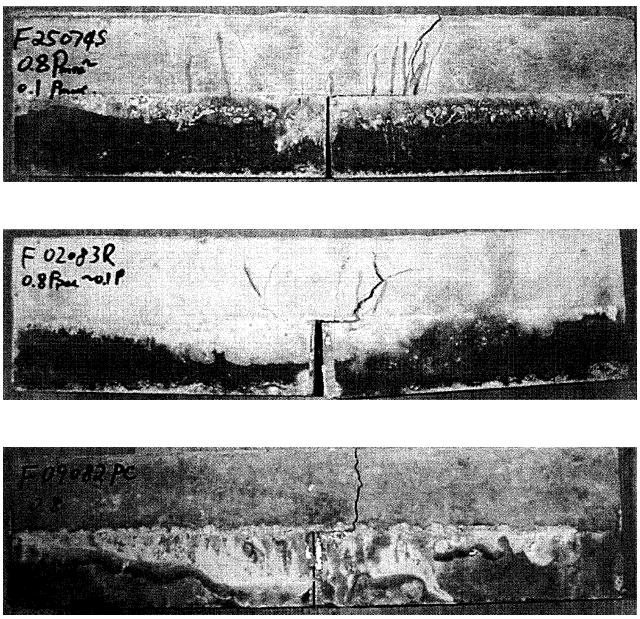

Fig. 9. Crack patterns at failure of overlaid beams under fatigue bending load: (a) ECC overlay with smooth casting surface, (b) ECC overlay with rough casting surface and (c) PC overlay with smooth casting surface.

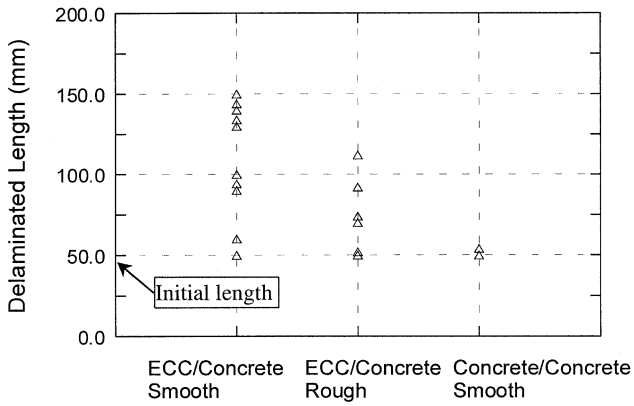

Fig. 10. Interfacial delaminating length in different types of beams under fatigue bending load.

stress versus fatigue life ($S-N$) diagrams. The typical crack patterns at failure of the beams with different overlay materials (PC and ECC) and different interfacial characteristics (smooth cut surface and rough sand-blasted surface) under fatigue loading are shown in Fig. 9. The delaminated length along the overlay/base concrete interface measured after testing under fatigue loading is shown in Fig. 10 and the corresponding deflections at fatigue failure are listed in Table 4.

From these test results, first, we can see that the fatigue life of the ECC/concrete composite beams is almost not influenced by the interfacial characteristics resulting from the procedure of concrete substrate surface preparation. That is because the flexural fatigue life of a beam is governed by a single dominated fatigue crack propagation behavior. No matter how many cracks are developed during fatigue loading, the number of fatigue cycles until failure is principally controlled by the crack bridging performance of the dominant single crack under cyclic loading [15,16]. However, the number of cracks developed during fatigue loading does influence the ultimate deformation level of the beam at fatigue failure. The more cracks developed during fatigue loading, the larger the deformation achieved at fatigue failure.

Due to the large difference between the ultimate flexural strength of PC and ECC overlaid beams (see Fig. 5),

Table 4
Deflections of the overlaid beams at fatigue failure

Specimen types	F_{max} (MPa)	Deflection at failure[a] (mm)
PC overlay with smooth interface	5.54 (0.8 MOR)	0.1
	4.85 (7 MOR)	0.2
ECC overlay with rough interface	10.86 (0.85 MOR)	1.45
	10.22 (0.8 MOR)	(1.30, 1.10) 1.20
ECC overlay with smooth interface	10.65 (0.9 MOR)	(1.92, 4.38) 3.15
	9.47 (0.8 MOR)	(1.80, 2.25) 2.03

[a] The value listed is measured based on position of machine actuator.

the load levels used on ECC overlaid beams were not applied on PC overlaid beams in the fatigue study. However, from Fig. 8, there is no doubt that under the same traffic load condition, the fatigue life of ECC overlaid beams can be significantly increased in comparison to that of PC overlaid beams.

By comparing Fig. 6 with Figs. 9, there is no obvious difference on the crack patterns at failure between monotonic and fatigue loading at the load level employed in these experiments. This result suggests that even though the fiber/matrix interface may suffer certain damage during fatigue loading leading to fiber bridging stress degradation [17,18], the fiber bridging stress is still sufficient to result in multiple cracking. However, this conclusion needs to be further confirmed by lower fatigue load level than that used in the current study.

4. Theoretical analyses of overlay behavior

The reasons why the ECC overlaid beams have much better performance than that of PC overlaid ones can be analyzed from two aspects regarding flexural strength and deformability. ECC is a micromechanically optimized composite and has a superior crack bridging behavior compared to that of PC and/or conventional fiber-reinforced concrete (FRC). It is well understood that the bending performance of a beam is strongly influenced by the stress–crack opening ($\sigma-\delta$) relationship of the material [13,14,19]. The theoretical model-predicted $\sigma-\delta$ relationships of PC [20] and PVA-ECC [21,22] used in the present study are shown in Fig. 11. As a comparison, the model-predicted $\sigma-\delta$ relationship of conventional steel FRC (SFRC) [15,23] is presented in the figure also. The detailed material parameters used in the theoretical $\sigma-\delta$ relationship can be found in the related reference list above. Corresponding to Fig. 11, Fig. 12 shows the model-predicted flexural stress versus crack mouth opening diagrams of overlaid beams using PC, SFRC and PVA-ECC as overlay materials, respectively, based on a fracture mechanical model [14]. From these predictions, it can be seen that the crack bridging behavior of ECC can lead to much better flexural performance in both flexural strength and CMOD at peak stress compared to PC and conventional SFRC. This indicates that by applying ECC in the layer, significant improvement in flexural strength over that of PC can be achieved. By comparing with the experimental results shown in Fig. 5, good agreement between model predictions and test results on MOR can be found.

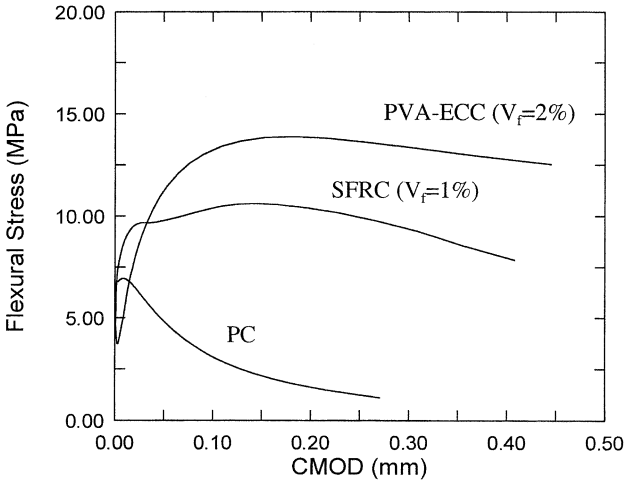

Fig. 12. Predicted flexural stress versus CMOD curves of overlaid beams with different overlay materials.

In terms of deformability, the superior crack bridging behavior of ECC material results in strain-hardening behavior accompanied by multiple cracking in tension. In contrast, conventional SFRC and PC show typically strain softening and single cracking behavior in tension. Typical experimentally determined tensile stress–strain curves of PVA-ECC [12], SFRC and PC [13,24] are shown in Fig. 13. The unique strain-hardening property leads to significantly

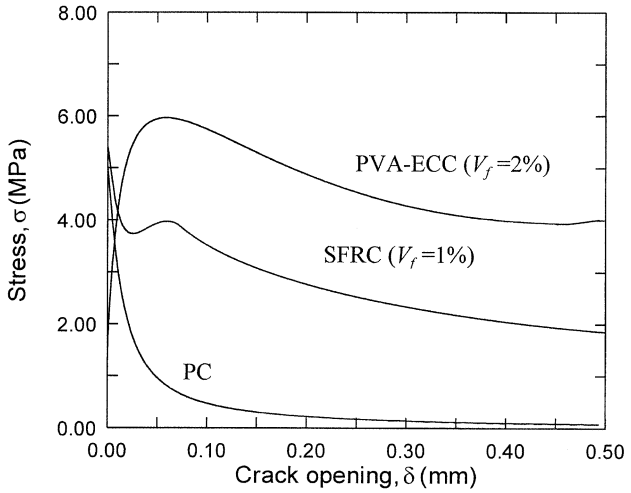

Fig. 11. Theoretical predicted stress–crack width relationship of PC, SFRC and PVA-ECC materials.

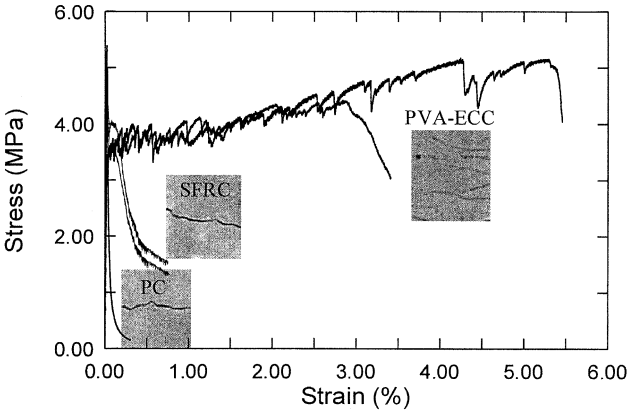

Fig. 13. Experimentally determined stress–strain relations of PVA-ECC, SFRC and PC materials in tension, showing multiple and single cracking behavior.

enhanced deformability of the ECC overlaid beams at peak load compared to that of PC and conventional SFRC overlaid beams. The flexure performance of SFRC overlaid beams can be found elsewhere [10,11]. This can be understood as the deformation capacity represented by deflection or tensile strain contributed by the opening of each individual microcrack. The more the number of microcracks, the larger the strain or deformation. In addition, the deformation capacity is also influenced by the microcrack width, which can be controlled by micromechanical fiber and fiber/matrix interfacial tailoring [8]. Finally, the number of microcracks in the ECC overlay is strongly influenced by the length of the zone maximum flexural stress that may develop in the layer, i.e., the length of delaminant zone along the ECC/concrete interface. Therefore, strong bond between ECC and concrete base, such as sand-blasted casting surface, will result in shorter delaminated zone and lead to small deformation at peak load than that in the case of smooth bond (see Figs. 5 and 7 for monotonic loading case and Fig. 9 for the fatigue case). This suggests that a certain length of initial unbonded zone along the ECC overlay and concrete subtract is needed to achieve required deformation level, such as shrinkage and temperature change-induced dimensional changes, without reducing the load carrying capacity and/or widening the crack width in the layer.

It may be expected that due to the stress concentration effect of the joint in the concrete substrate, the deformation behavior of the ECC overlaid pavements may consist of multiple microcracks as shown in Fig. 14. To prevent macrocrack localization, certain criteria on both ECC material property (tensile strain capacity typically) and the length of initial unbonded zone along the overlay/concrete substrate interface are needed. A representative length containing one joint is analyzed, where L is joint spacing and l is length of unbonded zone. Similar to the concept of ductile strips in bridge decks and concrete pavements proposed by Zhang et al. [24], the overall tensile strain capacity of the layer, ε_c, is reached when the stress in the microcracking zone reaches the tensile strength of ECC. Hence, ε_c is

$$\varepsilon_c = \varepsilon_I\left(\frac{l}{L}\right) + \varepsilon_{II}\left(1-\frac{l}{L}\right) \tag{2}$$

where ε_I is the strain capacity of cracked ECC and ε_{II} is the strain value of uncracked ECC at the load level of tensile

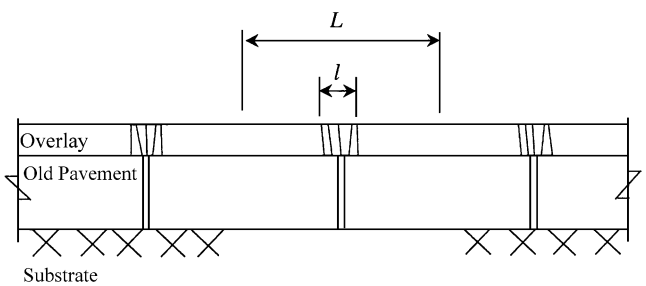

Fig. 14. Expected reflective crack patterns of ECC overlaid pavements.

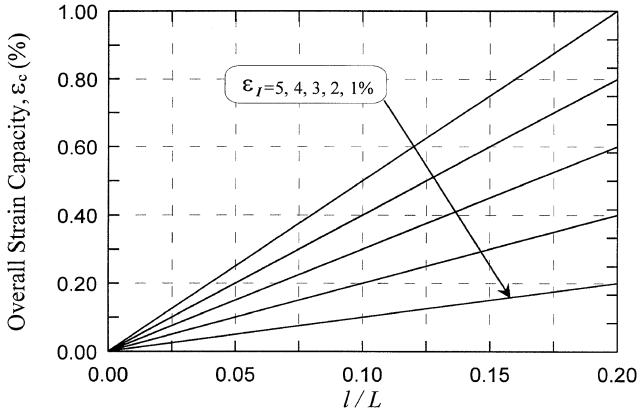

Fig. 15. Overall strain capacity as function of unbonded length and strain capacity of ECC material.

strength achieved in the cracked zone. Since $\varepsilon_I \varepsilon_{II}$, Eq. (2) can be simplified as (see Eq. (3))

$$\varepsilon_c = \varepsilon_I\left(\frac{l}{L}\right) \tag{3}$$

Therefore, the strain capacity, ε_c, is a function of ε_I and the ratio of l/L. For given material properties, ε_c is influenced only by the ratio of l/L. Fig. 15 demonstrates the overall strain capacity, ε_c, as a function of l/L for different strain capacity of ECC, ε_I. It clearly shows that for a given l/L, the higher the strain capacity of ECC, the higher the overall strain capacity of the layer. In addition, a prescribed overall strain capacity can also be obtained by adjusting the unbonded or delaminated length l. With a reasonable combination of length l and ε_I, it is possible to achieve a prescribed strain capacity requirement (imposed by shrinkage or temperature change or both), which may be 20 or 30 times of the strain capacity of PC without loss of load carrying capacity. In this case, deformation in the form of microcracking can only occur within the range of l when the structure is subject to tensile stress. The ECC within the unbonded area 'plastically' yields to accommodate the imposed strain.

5. Conclusions

The following conclusions can be drawn from the current experiments and theoretical analyzes:

1. When ECC is used as overlaid material over substrate concrete, both load carrying capacity and deformability of the overlaid composite beams in flexure are significantly increased compared to those of PC overlaid beams. The increase in deformability in the form of microcracking eliminates reflective cracking commonly observed in distressed pavements overlaid with conventional concrete. The increase in load carrying capacity can prolong the fatigue life of the structure under traffic loading.

2. The fatigue life of ECC overlaid beams in flexure is not influenced by the layer/base concrete interfacial

characteristics, such as smooth cutting surface or sand-blasted rough surface. However, the deformation capacity of the overlaid beams, represented by the deflection at midpoint of beam at peak load in the present paper, in both static and cyclic loading cases is influenced by the interfacial property. The smooth casting surface leads to larger deformation than that of rough casting surface.

3. A certain length of unbonded zone along the interface between the ECC overlay and old concrete substrate above existing old joints or cracks is required to achieve the needed deformation level of the layer. The required length of the unbonded zone is a function of the strain capacity of the ECC material. Debonding along the ECC/concrete interface is enhanced by the smooth cutting surface of the concrete substrate.

4. Due to the lower crack resistance of PC material and single cracking behavior in tension, the interfacial characteristics will not influence the deformation ability of the PC overlaid beams.

Acknowledgments

This work has been supported by a grant from the National Science Foundation (CMS-9872357) and the Kuraray (Osaka, Japan) to the University of Michigan. Support by Scientific Foundation for Returned Overseas Chinese Scholars, Ministry of Education, P.R.C. is acknowledged.

References

[1] B.O.A. Emmanuel, K. Lev, T.G. Leslie, Mechanistic-based model for predicting reflective cracking in asphalt concrete-overlaid pavements, Transp. Res. Rec. 1629 (1998) 234–241.
[2] S. Matsui, Technology developments for bridge decks — innovations on durability and construction (in Japanese), Kyouryou To Kiso 97 (8) (1997) 84–92.
[3] P.C. Perdikaris, S. Beim, Reinforced concrete bridge decks under pulsating and moving load, ASCE J. Struct. Eng. 114 (3) (1988) 591–607.
[4] P.C. Perdikaris, S.R. Beim, S.N. Bousias, Slab continuity effect on ultimate and fatigue strength of reinforced concrete bridge deck models, ACI Struct. J. 86 (4) (1989) 483–491.
[5] S.V. Kumar, H.V.S. GangaRao, Fatigue response of concrete decks reinforced with FRP rebars, ASCE J. Struct. Eng. 124 (1) (1998) 11–16.
[6] M.M. Szerszen, A.S. Nowak, L.J. Kwasniewski, Development of the procedure for efficient evaluation of bridge decks, UMCEE 99-14, Final Report, Dec. 1999.
[7] V.C. Li, From micromechanics to structural engineering — the design of cementitious composites for civil engineering applications, JSCE J. Struct. Mech. Earthquake Eng. 10 (2) (1993) 37–48.
[8] V.C. Li, Engineered cementitious composites — tailored composites through micromechanical modelling, in: N. Banthia, A. Bentur, A. Mufti (Eds.), Fiber Reinforced Concrete: Present and the Future, Canadian Society for Civil Engineering, Montreal, 1998, pp. 64–97.
[9] V.C. Li, Y.M. Lim, D.J. Foremsky, Interfacial fracture toughness of concrete repair materials, in: F.H. Wittman (Ed.), Proceedings of Fracture Mechanics of Concrete Structures II, Aedificatio Publishers, Freiburg, 1995, pp. 1329–1344.
[10] Y.M. Lim, V.C. Li, Durable repair of aged infrastructures using trapping mechanism of engineered cementitious composites, Cem. Concr. Compos. 19 (4) (1997) 373–385.
[11] T. Kamada, V.C. Li, The effect of surface preparation on the fracture behavior of ECC/concrete repair system, Cem. Concr. Compos. 22 (6) (2000) 423–431.
[12] V.C. Li, S. Wang, C. Wu, Tensile strain-hardening behavior of PVA-ECC, ACI Mater. J. (2000) (submitted for publication).
[13] J. Zhang, H. Stang, Application of stress crack width relationship in predicting the flexural behavior of fiber reinforced concrete, Cem. Concr. Res. 28 (3) (1998) 439–452.
[14] J. Zhang, V.C. Li, Modeling of mode I crack propagation in fiber reinforced concrete by fracture mechanics, Construction Materials — Theory and Application, Ibidem-Verlag, Stuttgart, 1999, pp. 215–228.
[15] J. Zhang, Fatigue fracture of fiber reinforced concrete — an experimental and theoretical study. PhD thesis, Department of Structural Engineering and Materials, Technical University of Denmark, Serie R, 41, 1998.
[16] J. Zhang, H. Stang, V.C. Li, Fatigue life prediction of fibre reinforced concrete under flexure load, Int. J. Fatigue 21 (10) (1999) 1033–1049.
[17] J. Zhang, H. Stang, Interfacial degradation in cement-based fiber reinforced composites, J. Mater. Sci. Lett. 16 (11) (1997) 886–888.
[18] J. Zhang, H. Stang, V.C. Li, Experimental study on crack bridging in FRC under uniaxial fatigue tension, ASCE J. Mater. Civ. Eng. 12 (1) (2000) 66–73.
[19] M. Maalej, V.C. Li, Flexural strength of fibre cementitious composites, J. Mater. Civ. Eng. 6 (3) (1994) 390–406.
[20] H. Stang, T. Aarre, Evaluation of crack width in FRC with conventional reinforcement, Cem. Concr. Compos. 14 (2) (1992) 143–154.
[21] Z. Lin, T. Kanda, V.C. Li, On interfacial property characterisation and performance of fiber reinforced cementitious composites, Concr. Sci. Eng., RILEM 1 (3) (1999) 173–184.
[22] C. Wu, Miromechanical tailoring on PVA-ECC materials. PhD thesis, Advanced Civil Engineering Materials Research Laboratory (ACE-MRL), Department of Civil and Environmental Engineering, University of Michigan, 2000.
[23] V.C. Li, H. Stang, H. Krenchel, Micromechanics of crack bridging in fiber reinforced concrete, Mater. Struct. 26 (1993) 486–494.
[24] J. Zhang, V.C. Li, A. Nowak, S. Wang, Introducing ductile strip for durability enhancement of concrete slabs, ASCE J. Mater. Civ. Eng. (2001) (in press).